Computers & Operations Research 39 (2012) 1173–1186

Contents lists available at ScienceDirect

Computers & Operations Research

journal homepage: www.elsevier.com/locate/caor

Simultaneous re-design and scheduling of multiple effect evaporator systems

Humberto Heluane [a], Aníbal M. Blanco [b], María Rosa Hernández [a], J. Alberto Bandoni [b,*]

[a] Departamento de Ingeniería de Procesos y Gestión Industrial, FACET, Universidad Nacional de Tucumán, Av. Independencia 1800, (4000) Tucumán, Argentina
[b] PLAPIQUI (UNS—CONICET), Camino La Carrindanga km. 7 (8000) Bahía Blanca, Argentina

ARTICLE INFO

Available online 13 July 2011

Keywords:
Evaporation
Re-design and scheduling
Mathematical programming
Sugar industry

ABSTRACT

Evaporation is a key operation in many industries and its optimization is required for the efficient management of water and energy within the process. During the operation, dissolved solids settle on the heat exchange surfaces with the consequent increase in the heat transfer resistance. Therefore, periodic shutdowns of the trains of evaporators are required for the cleaning of the units in order to restore acceptable performance. In this work the simultaneous re-design and scheduling of multiple effect evaporation systems is addressed. A mixed integer nonlinear programming model based on a discrete time representation is proposed and applied to a typical evaporation system in the sugar industry with several multiple effect parallel lines and time decaying performance.

1. Introduction

Evaporation is a key operation in many industrial processes. Typically, an evaporation network consists of several series (lines, trains) of evaporation units working in parallel.

Fouling is the process by which solid particles settle and accumulate on heat transfer surfaces. This phenomenon is particularly detrimental when the involved fluids contain large concentrations of dissolved or suspended matter since significant increases of the heat transfer resistance can take place in short periods of time. Consequences of fouling in process industries are increased energy consumption, extra maintenance and labor costs, and loss of production opportunities. In order to cope with fouling, equipment must be shut down and cleaned to restore the original operating efficiency.

Several works have proposed methods for the optimization of the cleaning schedules for single heat exchangers [1–3]. However, when multiple interconnected heat transfer units are used, the operating conditions of each exchanger affect the overall heat exchange performance. Therefore, a rational maintenance policy must be applied to the whole evaporation network in order to accomplish the desired production at a minimum cost.

Mathematical programming techniques have been used for the optimal planning and scheduling of both, batch and continuous processes, with time decaying performance. Georgiadis et al. [4] and Georgiadis and Papageorgiou [5] incorporated fouling models into the problem of maintenance scheduling of heat exchanger networks. In those studies, heat transfer rate decayed with time due to fouling. The scheduling of parallel evaporation lines has been addressed in Heluane et al. [6] and Heluane et al. [7], where loss of efficiency due to fouling was also considered. A similar problem arises in several other engineering systems that present time decaying performance processes, such as reactors with catalyst deactivation and cracking furnace fouling in ethylene plants [8–10].

Besides the fouling, it should be noticed that, since evaporators of different sizes can be present in an evaporation system, the design (configuration) of a network is a very important consideration since it affects the amount of required steam.

The design of evaporation systems involves the determination of the number of parallel trains and the number of units per train, together with the size (heat transfer area) of each unit, out of a discrete set of available sizes. The design problem is necessarily integrated with the operational scheduling of the system in order to optimize the net benefit of the operation.

In this contribution, a multi-period optimization model that addresses the simultaneous re-design and scheduling of multiple effect evaporation networks is presented. It is assumed that the units of a given evaporation network can be re-arranged to improve the overall operation of the system. In other words the re-design problem involves the configuration of a new network from a set of existing evaporators. The re-design problem can be considered as a particular case of the general design problem in which the network can be built up from commercially available equipment.

The performance criterion should be adopted in accordance with the studied process. Generally, it has to deal with the optimization of the steam consumption while ensuring certain target concentration. In many processes it is usually desired to generate cyclic cleaning schedules, which can be repeated over time.

* Corresponding author.
E-mail addresses: hheluane@herrera.unt.edu.ar (H. Heluane), ablanco@plapiqui.edu.ar (A.M. Blanco), rhernandez@herrera.unt.edu.ar (M.R. Hernández), abandoni@plapiqui.edu.ar (J.A. Bandoni).

0305-0548/$ - see front matter © 2011 Elsevier Ltd. All rights reserved.
doi:10.1016/j.cor.2011.06.015

Notation

A Heat exchange area (m^2)
C Cost ($)
c_s Specific steam cost ($/t)
$C1$, $C2$ Parameters of the global heat transfer resistance model
F Outlet liquid flow rate from an evaporation unit (t/h)
FI Inlet flow rate to an evaporation line (t/h)
$F0$ Total inlet flow rate (t/h)
FM Total outlet flow rate (t/h)
FO Objective function
$BM1$, $BM2$ Big-M constants
M General number of units in a line
N General number of parallel lines
NE Number of units in a line
p Operating pressure in a unit (mmHg)
p_S Pressure of steam (mmHg)
R Global heat transfer resistance (h m^2 °C/kcal)
R^0 Global heat transfer resistance for clean unit (h m^2 °C/kcal)
S_C Crystallization steam (t/h)
S_E Evaporation steam (t/h)
TC Shutdown period
V Vapor flow rate (t/h)
V_C Water removed as vapor from crystallization stage (t/h)
V_E Water removed as vapor from evaporation stage (t/h)
x Concentration (%)
x_M Evaporation outlet concentration (%)
x_P Crystallization outlet concentration (%)
x_0 Feed concentration (%)

Greek letters

λ Heat of vaporization (kcal/kg)
θ Operating temperature (°C)
Δp Pressure drop (mmHg)
$\Delta\theta$ Temperature difference (°C)

Indexes

h Cleaning shutdown
i Line (row)
j Position in a line (column)
m Cleaning shutdown
t Time period
w Unit

Binary variables

$a_{i,t}$, $b_{i,t}$ Auxiliary variables for defining z
$n_{i,j}$ Indicates is a position has a unit
$yn_{i,j,w}$ Indicates the position of a unit
$y_{m,i,j}$ Indicates if a line is shut down
yL_i Indicates if a line has units
$y0_i$, $y3_i$, $y4_i$, $y5_i$ Indicates the number of units in a line
$z_{h,i,t}$ Cleaning cycles

The resulting model is mixed integer nonlinear (MINLP) and it is applied in this work to the evaporation stage of a typical sugarcane process. For this particular case study, the global steam consumption, which also includes the crystallization stage, is optimized.

2. Description of the evaporation process

Evaporation is a special separation process where a volatile solvent is separated from a nonvolatile solute. Basically, a diluted stream ($F0$, x_0) is concentrated by evaporating a fraction of the solvent in one or several units arranged in series and parallel structures (Fig. 1) to obtain a concentrated product ($F_{i,M}$, $x_{i,M}$).

Evaporation is commonly found in the inorganic, organic, paper, and food industries. Typical applications include the concentration of sodium hydroxide, brine, organic colloids, and fruit juices. Generally, the solvent is water. In most cases the concentrate resulting from the evaporation process is the final product. Sometimes, however, the evaporated, volatile component is the main product, as for example, in water desalination.

Evaporation takes place in evaporators (Fig. 1). There are several commercially available evaporator types. In most designs, the heating medium (usually steam) flows and condensates inside a tubular coil, which is surrounded by the boiling liquid. The heat provided by the condensing steam evaporates some solvent of the boiling mixture, which concentrates in the dissolved component.

The energy consumption to evaporate a solution is fairly significant. Therefore, in order to reduce the energy cost, multiple effect evaporation arrangements are usually adopted. In multiple effect operation, several evaporators are connected in series where the product stream is pumped from unit to unit (Fig. 1). Steam is introduced to the heating coil of the first effect (evaporator). Upon condensing, the steam boils off a proportional amount of vapor that is used as heating medium for the following evaporation unit.

To provide the temperature potential required for the heat transfer to occur, it is necessary to operate each effect at successively lower pressures and, therefore, lower boiling temperatures. The rationale behind this practice roots in the significant dependence of the boiling point of a liquid with the pressure. This relationship is modeled by Antoine's equation, which is introduced later in this article.

For instance, the vapor that is generated in the first effect is injected into the heating coil of the second effect (Fig. 1). This second vessel operates at a lower pressure than the previous unit, so the boiling point of the liquid in the second effect is lower than the condensing temperature of the vapor leaving the first effect. Similarly, the vapor from the second effect becomes the heating medium to the third effect, and so on. The pressure drop from unit to unit depends on the pressure at which the last effect of the series is operated and on the number of units present in the line.

Finally, several multiple effect series are usually arranged in parallel (Fig. 1) to achieve product demand and also to allow equipment maintenance of individual lines without shutting down the whole evaporation process.

3. Mathematical formulation

The addressed problem can be defined as follows:
Given:

- Flow rate of material to be processed.
- Feed concentration.

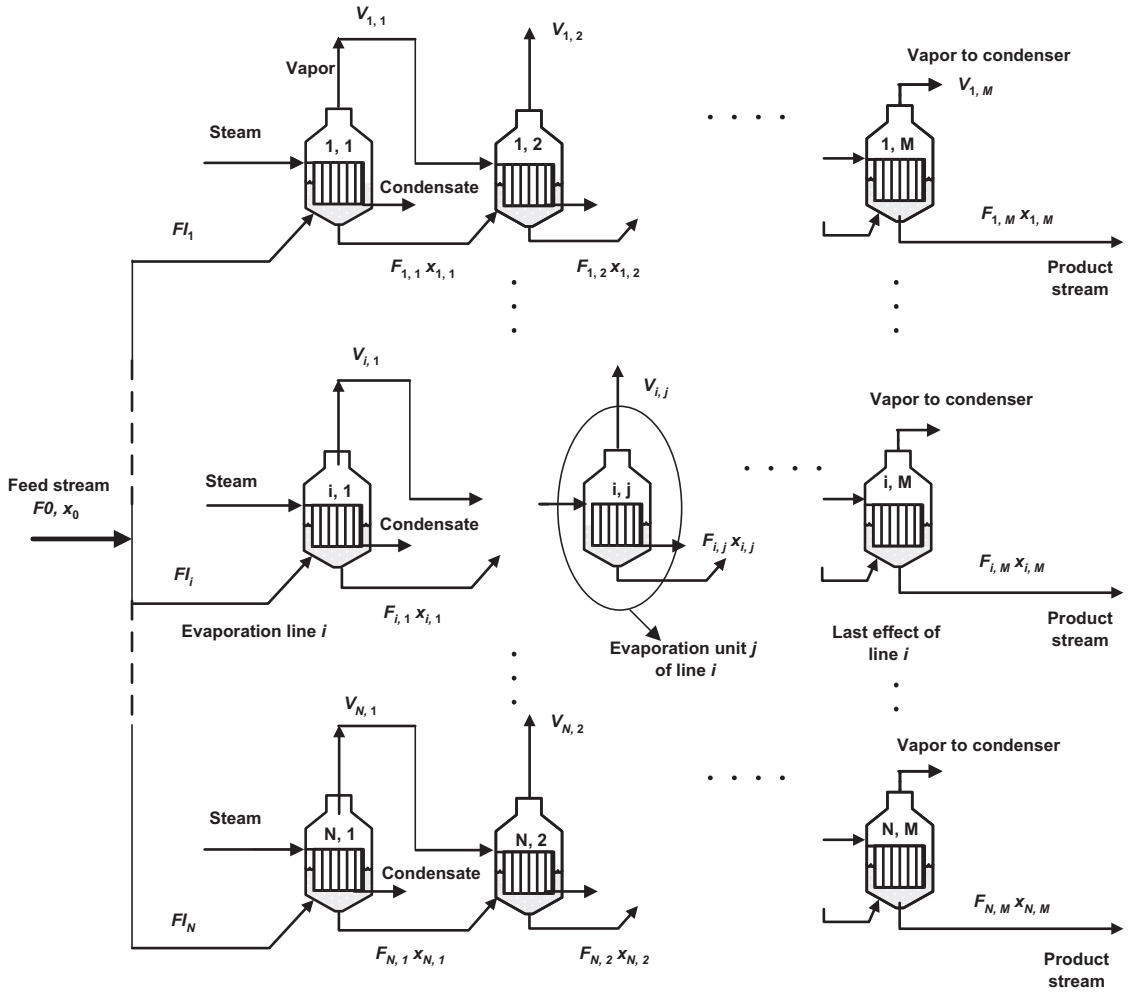

Fig. 1. Scheme of multiple effect evaporation lines working in parallel.

- Heat exchange area of the available evaporation units.
- Heat transfer resistance increase rate for each unit.
- Heat transfer resistance value for each unit at time zero.

Determine:

- Configuration of the evaporation network.
- Lines shut down scheduling for cleaning purposes.
- Time profiles of concentrations and flow rates.

3.1. Model assumptions

The following assumptions have been considered to derive the model presented in this work:

(i) Negligible boiling point increase at the evaporator units.
(ii) No solute loss in the system.
(iii) Linear pressure drop among all the evaporation units of a line.
(iv) Constant conditions at the evaporation units during operation.

3.2. Re-design subproblem

Given a set W of evaporation units, they can be arranged on a network as the one shown in Fig. 1. The network is conceptualized as a matrix of N rows (lines) and M columns.

Each unit w of set W can be assigned to a position (i,j) using a binary variable $yn_{i,j,w}$, which is defined to be 1 when unit w is placed in position (i,j) and 0 otherwise.

Eq. (1) ensures that each position (i,j) must be occupied (if occupied) by only one unit w.

$$\sum_{w=1}^{W} yn_{i,j,w} \le 1 \quad \forall i,j \tag{1}$$

Eq. (2) ensures that each evaporation unit is used only once in the network.

$$\sum_{i=1}^{N}\sum_{j=1}^{M} yn_{i,j,w} = 1 \quad \forall w \tag{2}$$

The heat exchange area (A_w) is the characteristic parameter of an evaporation unit. A new variable $A_{i,j}$ is used to represent that unit w of area A_w is placed in position (i,j). Eq. (3) is used to assign the value A_w to the corresponding $A_{i,j}$ variable. When $yn_{i,j,w}$ is equal to 1, evaporation unit w is placed in position (i,j) and, therefore $A_{i,j}=A_w$.

$$A_{i,j} = \sum_{w=1}^{W} A_w yn_{i,j,w} \quad \forall i,j \tag{3}$$

Eq. (4) is used to calculate the number of units (NE_i) present in each line.

$$NE_i = \sum_{j=1}^{M}\sum_{w=1}^{W} yn_{i,j,w} \quad \forall i \tag{4}$$

Binary variable $n_{i,j}$ is equal to 1 when the position (i,j) is occupied with a unit, and it is equal to 0 when the position is empty. Eq. (5) is used to define $n_{i,j}$.

$$n_{i,j} = \sum_{w=1}^{W} yn_{i,j,w} \quad \forall i,j \tag{5}$$

To ensure that there are no "gaps" in a line, i.e., to prevent the model from placing a unit in positions 1 and 3, with no unit in position 2, the following equation is used:

$$\sum_{w=1}^{W} yn_{i,j,w} \geq \sum_{w=1}^{W} yn_{i,j+1,w} \quad \forall i,j = 1,2,\ldots,NE^{max}-1 \tag{6}$$

where NE^{max} is the maximum number of allowed units in a line.

Finally, to take into account the possibility that a line of the matrix could result empty (no equipment assigned to that line) a new binary variable (yL_i) is defined as follows: $yL_i=0$ when line i has no equipment assigned and $yL_i=1$ otherwise. Thus, the number of units of a line is determined by Eqs. (7) and (8), where NE^{min} is the minimum number of allowed units in a line.

$$NE_i \geq NE^{min} yL_i \quad \forall i \tag{7}$$

$$NE_i \leq NE^{max} yL_i \quad \forall i \tag{8}$$

3.3. Mass and energy balances

The multi-period formulation based on a discrete time representation requires the definition of fixed number of periods, t, to model the system along the time horizon.

The following equation ensures that the whole mass flow rate fed to the evaporation system is processed:

$$F0 = \sum_{i=1}^{N} FI_{i,t} \quad \forall t \tag{9}$$

where $F0$ is the mass flow rate fed to the evaporation system and $FI_{i,t}$ is the mass flow rate fed to line i in period t.

Mass balances for the units of the evaporation lines are described by Eqs. (10)–(13).

$$FI_{i,t} = F_{i,j,t} + V_{i,j,t} \quad \forall i,t,j = 1 \tag{10}$$

$$x_0 FI_{i,t} = x_{i,j,t} F_{i,j,t} \quad \forall i,t,j = 1 \tag{11}$$

$$F_{i,j-1,t} = F_{i,j,t} + V_{i,j,t} \quad \forall i,t,j > 1 \tag{12}$$

$$x_{i,j-1,t} F_{i,j-1,t} = x_{i,j,t} F_{i,j,t} \quad \forall i,t,j > 1 \tag{13}$$

where $F_{i,j,t}$ and $x_{i,j,t}$ are the mass flow rate and concentration, respectively, of the stream leaving evaporator (i,j) in period t, $V_{i,j,t}$ is the vapor generated in evaporator (i,j) in period t, and x_0 is the concentration of the feed stream.

When a line i is operating, the vapor generated in each unit is calculated from the energy balance as follows:

$$V_{i,j,t} = \frac{A_{i,j}\Delta\theta_{i,j}}{\lambda_{i,j}} \frac{1}{R_{i,j,t}} \quad \forall i,j,t \tag{14}$$

where $\Delta\theta_{i,j}$ stands for the temperature difference in each unit, which is the driving force for the evaporation work, $R_{i,j,t}$ is the global heat transfer resistance, which varies with time due to fouling, and $\lambda_{i,j}$ is the latent heat of vaporization of the boiling liquid. Eq. (14) is obtained by equalizing the vaporization heat of the boiling liquid, $Q=\lambda V$, and the heat provided by transference through the coils: $Q=A\Delta\theta/R$.

Since pressure and boiling temperature decrease along the evaporation line as the product is concentrated, the operating conditions of each evaporation unit depends on its relative position in the line. On the other hand, the number of units in the line also determines their operating conditions because the total pressure drop of the line is distributed among them. Considering a linear pressure drop along the evaporation line, the pressure drop in each evaporator is given by

$$\Delta p_{i,j} = \frac{\Delta p}{NE_i} \quad \forall i,j \tag{15}$$

where Δp is the total pressure drop, which is defined as the difference between the pressure of the steam used in the first unit and the working pressure in the last unit of a line [11]. The operating pressure of each unit is therefore calculated as follows:

$$p_{i,j} = p_s - n_{i,j} \frac{\Delta p}{NE_i} \quad \text{if } j = 1 \quad \forall i \tag{16}$$

$$p_{i,j} = p_{i,j-1} - n_{i,j} \frac{\Delta p}{NE_i} \quad \text{if } j > 1 \quad \forall i \tag{17}$$

Saturation temperature is calculated with Antoine's equation using water parameters in the range 11–168 °C [12].

$$\ln p = 18.30 - \frac{3816.44}{\theta + 227.02} \tag{18}$$

where pressure p is expressed in mmHg, and temperature θ in °C. The latent heat of vaporization (λ) in kcal/kg is calculated with the Watson expression [12]:

$$\lambda = 748\left[1 - \frac{\theta + 273.15}{647.10}\right]^{0.38} \tag{19}$$

To ensure that enough vapor is available for the second unit of a line, the amount of heat generated at the first unit must be greater than or equal to the heat required by the second evaporator:

$$\lambda_1 V_1 \geq \lambda_2 V_2 \tag{20}$$

When vapor V_1 is not completely condensed at the second evaporator, the excess of energy $(\lambda_1 V_1 - \lambda_2 V_2)$ is available to be used in the third and following units. Also V_2 can be used as heating fluid for the third unit. This can be expressed as follows:

$$(\lambda_1 V_1 - \lambda_2 V_2) + \lambda_2 V_2 \geq \lambda_3 V_3 \tag{21}$$

By operating with Eq. (21)

$$\lambda_1 V_1 \geq \lambda_3 V_3 \tag{22}$$

Similar expressions can be obtained for the following units of an evaporation line

$$\lambda_1 V_1 \geq \lambda_j V_j \quad \forall j > 1 \tag{23}$$

Availability of vapor for the proper operation of an evaporation line is therefore ensured with the use of Eq. (23). When several lines are operating in parallel, generated vapors of the same level of energy are collected in a single pipe and then diverted to be used in other units. Therefore, the above equations can be generalized for N lines operating in parallel as follows:

$$\lambda_1 \sum_{i=1}^{N} V_{i,1} \geq \lambda_j \sum_{i=1}^{N} V_{i,j} \quad \forall j > 1 \tag{24}$$

Inequalities (25)–(27) ensure that mass flow rates and concentrations are equal to zero for an empty line (no units assigned to the line). F_i^{up} is the upper bound for the mass flow rate that can be processed in a line i and x_i^{up} is the maximum concentration that can be manipulated in the evaporation system.

$$FI_{i,t} \leq F_i^{up} yL_i \quad \forall i,t \tag{25}$$

$$F_{i,j,t} \leq F_i^{up} yL_i \quad \forall i,j,t \tag{26}$$

$$x_{i,j,t} \leq x_i^{up} yL_i \quad \forall i,j,t \tag{27}$$

3.4. Cleaning scheduling subproblem

Besides the re-design of the network, the other aim of the model is to determine the shutdown scheduling of the lines to perform the cleaning of the units.

In this work, the global heat transfer resistance increment due to fouling in each unit was considered to depend on its position in the train and to follow a linear relationship with time.

Fouling is a complex phenomenon, which is difficult to model for the general case, since it heavily depends on the involved components, concentrations, temperature levels, equipment design, operation time, etc. Several authors have studied fouling assuming different decaying performance profiles [5,13]. However, theoretical analysis [14] as well as practical evidence [15,16] supports the use of time dependent linear models. However, if for a particular case the behavior of the global heat transfer resistance is known to be nonlinear, the linear expression could be replaced by the appropriate model in the corresponding equations and the optimization can still be performed with the proposed strategy.

There are several possible strategies for the cleaning scheduling of the system. One possibility is to always have exactly $N-1$ trains working while one is shut down for cleaning. Once cleaned, the train is put back to work while another is shut down for maintenance. Other strategy considers the use of some storage capacity. Once a line is shut down for cleaning, a fraction of the incoming flow rate is temporarily stored in a tank. When the line is put back in operation and all the trains are working simultaneously, the processing capacity is larger than the incoming flow rate and the tank empties. This strategy allows the N trains to work simultaneously until one of them requires maintenance. Finally, it is also possible to distribute the incoming flow rate among the operative trains in every period. Once a train is shut down for cleaning purposes, the corresponding flow rate is distributed between the operative lines. This strategy also allows the N lines to be simultaneously operative when no cleaning tasks are being performed and does not require the use of storage tanks. The last strategy is adopted in this study.

The shutdown scheduling was modeled with the aid of binary variables according to the logic proposed in Houze et al. [9] and also used in Shulz et al. [10]. In order to model the decaying performance of the units with time due to fouling, a continuous variable $R_{i,j,t}$ is used. $R_{i,j,t}$ represents the global heat transfer resistance for unit (i,j) at time period t. Eq. (28) is used to model $R_{i,j,t}$ in this work.

$$R_{i,j,t} = C1_{i,j} + C2_{i,j}t \tag{28}$$

where $C1_{i,j}$ is the initial global heat transfer resistance of unit (i,j) and $C2_{i,j}$ is the fouling rate. In particular, when the evaporator is clean $C1_{i,j}$ is equal to $R^0_{i,j}$.

In order to model a cyclic cleaning schedule, binary variable $z_{h,i,t}$ is defined, whose logic is illustrated in Fig. 2. Variables $z_{h,i,t}$ are defined by Eqs. (29)–(41). In all cases BM stands for big-M constant.

$TC_{h,i}+1$ is the time period when cleanup number h for line i takes place. If time period t is lower than or equal to $(TC_{1,i}+1)$ then $z_{1,i,t}$ is equal to 1; otherwise, it is equal to 0.

$$t \le TC_{1,i}+1+BM1(1-z_{1,i,t}) \quad \forall i,t \tag{29}$$

$$t \ge TC_{1,i}+2-BM1z_{1,i,t} \quad \forall i,t \tag{30}$$

Binary variables $z_{2,i,t}$ are equal to 1 for time intervals between the first and second shutdown periods for evaporation line i, i.e., $(TC_{1,i}+2) \le t \le (TC_{2,i}+1)$; otherwise they are equal to 0.

$$t \ge TC_{1,i}+2-BM1(1-z_{2,i,t}) \quad \forall i,t \tag{31}$$

$$t \le TC_{1,i}+1+BM1a_{i,t} \quad \forall i,t \tag{32}$$

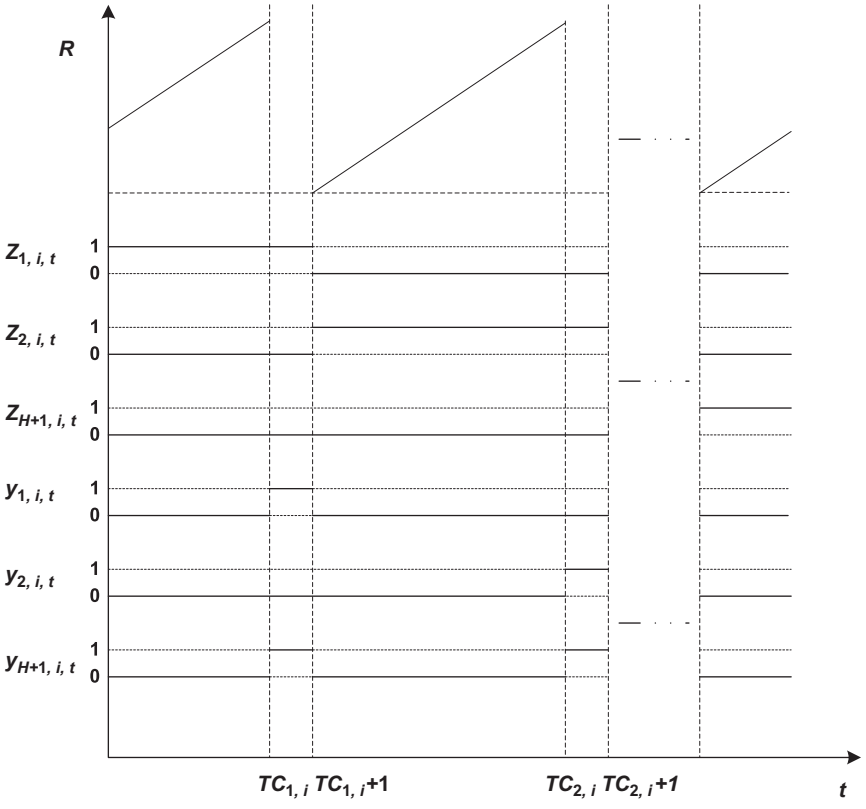

Fig. 2. Heat transfer resistance and binary variables $z_{h,i,t}$ and $y_{m,i,t}$.

$$t \geq TC_{1,i} + 2 - BM1(1-a_{i,t}) \quad \forall i,t \tag{33}$$

$$t \leq TC_{2,i} + 1 + BM1(1-z_{2,i,t}) \quad \forall i,t \tag{34}$$

$$t \leq TC_{2,i} + 1 + BM1(1-b_{i,t}) \quad \forall i,t \tag{35}$$

$$t \geq TC_{2,i} + 2 - BM1\ b_{i,t} \quad \forall i,t \tag{36}$$

To define $z_{2,i,t}$ it is necessary to introduce auxiliary binary variables $a_{i,t}$ and $b_{i,t}$, which are defined as follows: if $a_{i,t}=1$ and $b_{i,t}=1$ then $z_{2,i,t}=1$. When either $a_{i,t}=0$ or $b_{i,t}=0$ then $z_{2,i,t}=0$. Expressions (37)–(39) model such logic propositions. Fig. 3 shows how $a_{i,t}$ and $b_{i,t}$ shift from 0 to 1.

$$1 - a_{i,t} - b_{i,t} + z_{2,i,t} \geq 0 \quad \forall i,t \tag{37}$$

$$a_{i,t} - z_{2,i,t} \geq 0 \quad \forall i,t \tag{38}$$

$$b_{i,t} - z_{2,i,t} \geq 0 \quad \forall i,t \tag{39}$$

Analogous expressions are used to model more shutdown periods (third, fourth, etc.). For the last shutdown (H), a new binary variable $z_{H+1,i,t}$ is defined. For time intervals after the last shutdown, i.e., $t \geq TC_{H,i}+1$, binary variable $z_{H+1,i,t}$ is equal to 1, otherwise it is equal to 0.

$$t \leq TC_{H,i} + 1 + BM1\ z_{H+1,i,t} \quad \forall i,t \tag{40}$$

$$t \geq TC_{H,i} + 2 - BM1(1-z_{H+1,i,t}) \quad \forall i,t \tag{41}$$

For any time interval t, each evaporation line can only be in one state h.

$$\sum_{h=1}^{H+1} z_{h,i,t} = 1 \quad \forall i,t \tag{42}$$

The behavior of the global heat transfer resistance for the different periods t is modeled by the following inequalities. For time periods before or equal to $TC_{1,i}$ the values of $R_{i,j,t}$ are determined by Eqs. (43) and (44):

$$R_{i,j,t} \geq C1_{i,j} + C2_{i,j}t - BM1(1-z_{1,i,t}) \quad \forall i,j,t \tag{43}$$

$$R_{i,j,t} \leq C1_{i,j} + C2_{i,j}t + BM1(1-z_{1,i,t}) \quad \forall i,j,t \tag{44}$$

For time periods between the first and the second shutdowns $(TC_{1,i}+1) \leq t \leq TC_{2,i}$, the values of $R_{i,j,t}$ are calculated by Eqs. (45) and (46)

$$R_{i,j,t} \geq R^0_{i,j} + C2_{i,j}[t-(TC_{1,i}+1)] - BM1(1-z_{2,i,t}) \quad \forall i,j,t \tag{45}$$

$$R_{i,j,t} \leq R^0_{i,j} + C2_{i,j}[t-(TC_{1,i}+1)] + BM1(1-z_{2,i,t}) \quad \forall i,j,t \tag{46}$$

For time intervals between the second and third shutdowns, third and fourth shutdowns, etc., the values of $R_{i,j,t}$ are calculated with equations analogous to (45) and (46).

Finally, for periods after the last shutdown ($t \geq TC_{H,i}+1$), values of $R_{i,j,t}$ are determined by Eqs. (47) and (48).

$$R_{i,j,t} \geq R^0_{i,j} + C2_{i,j}[t-(TC_{H,i}+1)] - BM1(1-z_{H+1,i,t}) \quad \forall i,j,t \tag{47}$$

$$R_{i,j,t} \leq R^0_{i,j} + C2_{i,j}[t-(TC_{H,i}+1)] + BM1(1-z_{H+1,i,t}) \quad \forall i,j,t \tag{48}$$

The operation of each evaporation line will be stopped for cleaning when a certain level of fouling has been reached. For example, the second shutdown will occur when the global heat transfer resistances $R_{i,j,TC2}$ reach the value of $R_{i,j,TC1}$. The following equations define the shutdown periods with a small tolerance on the value of the resistances:

$$C1_{i,j} - R^0_{i,j} + C2_{i,j}(1 + 2TC_{1,i} - TC_{2,i}) \leq 0.0001 \quad \forall i,j \tag{49}$$

$$C1_{i,j} - R^0_{i,j} + C2_{i,j}(1 + 2TC_{1,i} - TC_{2,i}) \geq -0.0001 \quad \forall i,j \tag{50}$$

Analogous expressions can be used to determine third, fourth, etc., shutdown periods. To ensure that the operating cycles are performed, the model imposes that the global heat transfer resistances are lower than the maximum attained values for each line, both at the beginning ($t=1$) and at the end ($t=T$) of the time horizon. This is modeled by Eqs. (51) and (52).

$$R_{i,j,1} \leq C1_{i,j} + C2_{i,j}TC_{1,i} \quad \forall i,j \tag{51}$$

$$R_{i,j,T} \leq C1_{i,j} + C2_{i,j}TC_{H,i} \quad \forall i,j \tag{52}$$

In order to produce a cyclic cleaning schedule that can be repeated sequentially, it is enforced that the global heat transfer resistance in each unit at the end of the scheduling horizon equals its initial value. This is imposed by Eqs. (53) and (54) within a certain tolerance

$$R_{i,j,T} - C1_{i,j} \leq 0.0001 \quad \forall i,j \tag{53}$$

$$R_{i,j,T} - C1_{i,j} \geq -0.0001 \quad \forall i,j \tag{54}$$

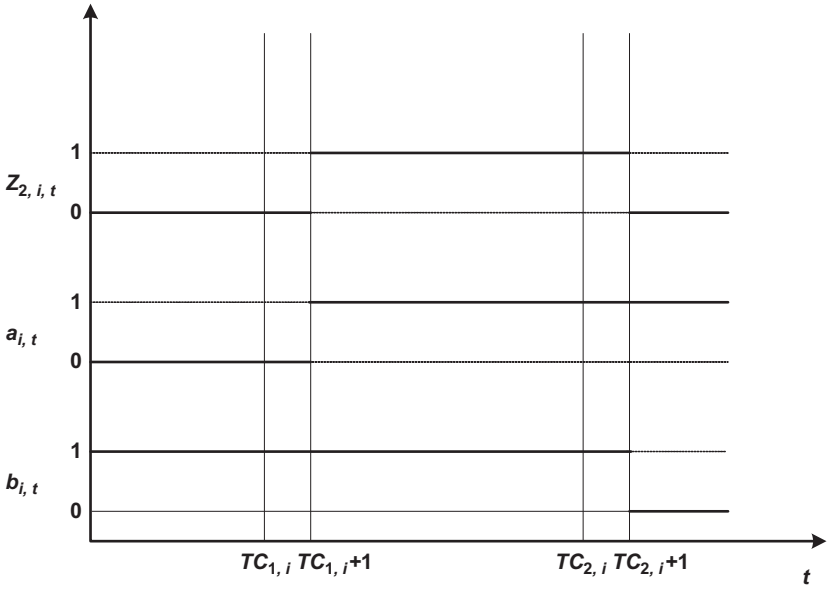

Fig. 3. Definition of variables $z_{2,i,t}$, $a_{i,t}$, and $b_{i,t}$.

Finally, a second set of binary variables, $y_{m,i,t}$, (Fig. 2) is used to define $TC_{h,i}$ and to make continuous variables associated to each evaporation line equal to zero during shutdown periods. Variable $y_{m,i,t}$ is equal to 1 if evaporation line i is shutdown in time period t, otherwise it is equal to 0.

$$TC_{h,i} = \sum_t (t-1) y_{m,i,t} \quad \forall i, h = 1,2,\ldots,H, \quad m = 1,2,\ldots,H \tag{55}$$

Binary variable $y_{H+1,i,t}$ is defined such that it is equal to 1 when any $y_{m,i,t}=1$ for $m=1,2,\ldots,H$ and is equal to 0 only when every variable $y_{m,i,t}$ is equal to 0 (see Fig. 2). The mathematical expressions for those propositions are given by inequalities (56) and (57).

$$y_{H+1,i,t} - y_{m,i,t} \geq 0 \quad \forall i,t,m = 1,2,\ldots,H \tag{56}$$

$$\sum_{m=1}^{H} y_{m,i,t} - y_{H+1,i,t} \geq 0 \quad \forall i,t \tag{57}$$

To impose H shutdowns in the time horizon, the following constraints are included in the model.

$$\sum_t y_{m,i,t} = 1 \quad \forall i,t, \quad m = 1,2,\ldots,H \tag{58}$$

The equation below ensures that each shutdown of a line is done in only one period t.

$$\sum_{m=1}^{H} y_{m,i,t} \leq 1 \quad \forall i,t \tag{59}$$

It is assumed that the available cleaning resources (especially manpower) allow the cleaning of only one line at a time. Such constraint is modeled by Eq. (60).

$$\sum_{i=1}^{N} \sum_{m=1}^{2} y_{m,i,t} \leq 1 \quad \forall t \tag{60}$$

The inequalities below force mass flow rates and concentrations to be equal to zero when a line i is being cleaned.

$$x_{i,j,t} \leq BM2(1 - y_{H+1,i,t}) \quad \forall i,j,t \tag{61}$$

$$FI_{i,t} \leq F_i^{up}(1 - y_{H+1,i,t}) \quad \forall i,t \tag{62}$$

$$F_{i,j,t} \leq F_i^{up}(1 - y_{H+1,i,t}) \quad \forall i,j,t \tag{63}$$

When a line i is operating ($y_{H+1,i,t}=0$ and $yL_i=1$), the vapor generated in the evaporation units is calculated from the energy balance by the following equations:

$$V_{i,j,t} \geq \frac{A_{i,j}\Delta\theta_{i,j}}{\lambda_{i,j}} \frac{1}{R_{i,j,t}} - BM2\, y_{H+1,i,t} - BM1(1 - yL_i) \quad \forall i,j,t \tag{64}$$

$$V_{i,j,t} \leq \frac{A_{i,j}\Delta\theta_{i,j}}{\lambda_{i,j}} \frac{1}{R_{i,j,t}} + BM2\, y_{H+1,i,t} + BM1(1 - yL_i) \quad \forall i,j,t \tag{65}$$

4. Evaporation in the sugar industry

While the formulation presented in the previous section is suitable for many evaporation systems, specific issues may arise in particular industries. Besides, while the design of the evaporation network might be set up to optimize a typical economic criterion (benefits minus capital and operative costs), the fact that evaporation is usually an intermediate stage within larger processes, generally prevents the formulation of a sound objective function for the isolated system. In order to illustrate the performance of the proposed model, a typical evaporation network of the sugar industry is considered as case study in this contribution. The developed framework can be applied with appropriate modifications to other processes as well. Moreover, fouling is particularly aggressive in the evaporation of the sugary liquor due to the highly viscous nature of the fluid and therefore represents an interesting application for the proposed approach.

Evaporation is used in the sugar manufacturing to concentrate the clarified juice prior to the crystallization stage. The aim of the evaporation and crystallization sections in a sugar factory is to eliminate water from the sugary juice in order to obtain crystals of sucrose. A basic scheme of the evaporation and crystallization sections of a sugar plant is shown in Fig. 4.

The evaporation process is energetically more efficient than the crystallization process due to the multiple effect arrangement. In a multiple effect series of M evaporators, the water extracted is approximately M times the steam injected to the first evaporator.

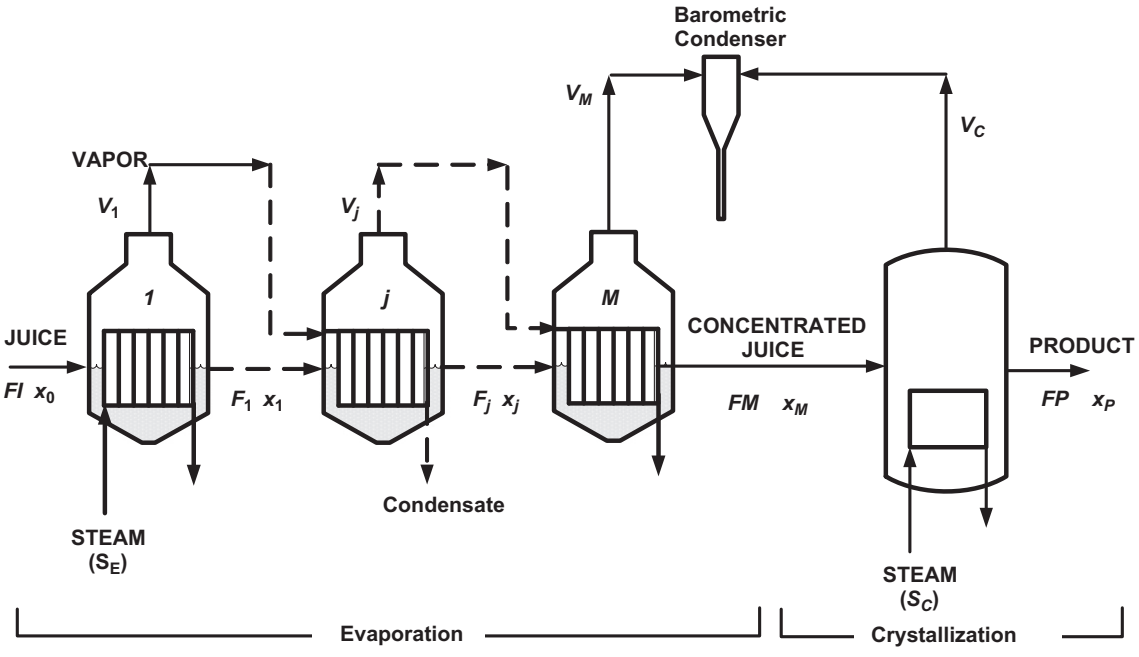

Fig. 4. Multiple effect evaporation and crystallization stages.

On the other hand, at the crystallization stage the water is extracted roughly in a proportion 1:1 with the consumed steam.

It is important therefore, to consider both, the evaporation and the crystallization stages for cost studies in the sugar industry. Considering that cleaning costs (due to fouling) are usually negligible compared with steam costs, the objective function to be minimized can be represented by the following equation:

$$C = C_{Cleaning} + C_{Steamforevaporation} + C_{Steam\ \ for\ \ crystallization} \cong c_S(S_E + S_C) \tag{66}$$

where S_E and S_C are the amounts of steam used at the evaporation and crystallization stages, respectively, and c_s is the specific steam cost. In multiple effect evaporators with M units, the water removed as vapor (V_E) is approximately:

$$V_E = MS_E \tag{67}$$

Such simplification relies on the assumption that the latent heat of vaporization is constant within the operating conditions of the system. For simplicity, in this study such assumption is adopted by neglecting the mild nonlinearity introduced by Eq. (19).

From the global mass balances for the evaporation section (Fig. 4)

$$x_0 FI = x_M FM \Rightarrow FM = \frac{x_0 FI}{x_M} \tag{68}$$

$$FI = FM + V_E \tag{69}$$

where x_M is the concentration of the juice leaving the evaporation line.

From Eqs. (67)–(69)

$$FI = \frac{x_0 FI}{x_M} + MS_E \tag{70}$$

Solving for S_E:

$$S_E = \frac{FI}{M}\left(1 - \frac{x_0}{x_M}\right) \tag{71}$$

From the global balances at the crystallization stage:

$$x_M FM = x_P FP \tag{72}$$

where x_P is the concentration of the product of the crystallization stage.

$$FM = FP + V_C \Rightarrow FP = FM - V_C \tag{73}$$

Taking into account that in the crystallization the vapor produced is equal to the condensed steam, $V_C = S_C$, and using expression (68) for FM, it is possible to calculate the steam required for crystallization as

$$S_C = FIx_0\left(\frac{x_P - x_M}{x_P x_M}\right) \tag{74}$$

By substituting expressions (71) and (74) in Eq. (66), the cost of the steam of the combined evaporation–crystallization section of the sugar plant is given by

$$C = c_s FI\left(\frac{x_P - x_0}{Mx_P} + \frac{x_0}{x_M}\left(\frac{M-1}{M}\right)\right) \tag{75}$$

Note from Eq. (75) that for a given configuration of the evaporation line, all the parameters are constant, except x_M. Therefore, the minimum overall operating cost will be obtained by maximizing this concentration, as can be seen from Fig. 5. In Fig. 5 the steam consumed in each section is plotted against the product concentration from the evaporation line for typical figures of the parameters. A measure of the sugar concentration x_M is therefore adopted here as the objective function.

A further simplification can be introduced based on the fact that the usual practice in the sugar industry is to configure lines with no more than five units and no less than three. Since Eq. (18) introduces severe nonlinearity within the model, pressure drops and temperature differences in each unit can be pre-calculated for three, four, and five unit arrangements and then assigned to the specific units by means of additional equations. In Tables 1–3 the driving force ($\Delta\theta$) for each evaporation unit is calculated for each line configuration considering a steam pressure of 1.56 atm (1185.60 mmHg) and a total pressure drop of 1.40 atm.

In order to assign the corresponding $\Delta\theta$ to each unit depending on the number of evaporators in a line, binary variables $y3_i$, $y4_i$, $y5_i$ are defined. Such variables are equal to 1 if there are 3, 4, or 5 units in line i, respectively, and 0 otherwise. Additionally,

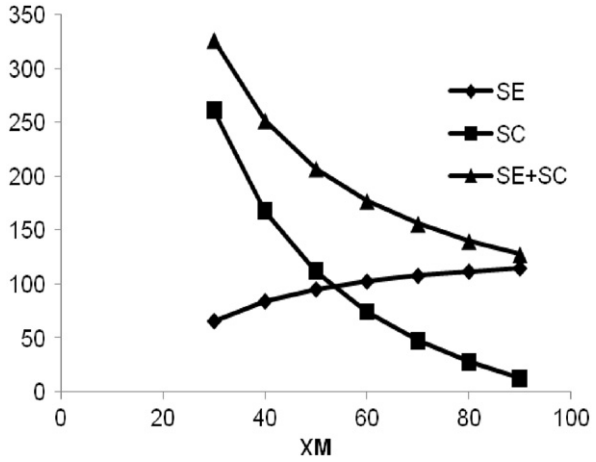

Fig. 5. Steam consumption in evaporation and crystallization.

Table 1
Parameters for a three units line.

	P (mmHg)	**T (°C)**	**Δθ3**
Steam	1185.60	112.97	
Unit 1	830.93	102.53	10.44
Unit 2	476.26	87.42	15.11
Unit 3	121.60	55.63	31.79

Table 2
Parameters for a four units line.

	P (mmHg)	**T (°C)**	**Δθ4**
Steam	1185.60	112.97	
Unit 1	919.60	105.44	7.53
Unit 2	653.60	95.84	9.60
Unit 3	387.60	82.17	13.67
Unit 4	121.60	55.63	26.55

Table 3
Parameters for a five units line.

	P (mmHg)	**T (°C)**	**Δθ5**
Steam	1185.60	112.97	
Unit 1	972.80	107.08	5.89
Unit 2	760.00	100.01	7.07
Unit 3	547.20	91.06	8.95
Unit 4	334.40	78.52	12.54
Unit 5	121.60	55.63	22.89

variable $y0_i$ is equal to 1 if there is no unit in line i and is 0 otherwise. Variables $y0_i$, $y3_i$, $y4_i$, and $y5_i$ are used in the following equations:

$$\Delta\theta_{i,j} = y0_i\Delta\theta0_j + y3_i\Delta\theta3_j + y4_i\Delta\theta4_j + y5_i\Delta\theta5_j \quad \forall i,j \tag{76}$$

$$y0_i + y3_i + y4_i + y5_i = 1 \quad \forall i \tag{77}$$

$$NE_i = 0y0_i + 3y3_i + 4y4_i + 5y5_i \quad \forall i \tag{78}$$

This strategy avoids some nonlinearity at the expense of the inclusion of additional binary variables. However, it should be noticed that the model remains MINLP due to the nonlinearities introduced by the mass balances in Eqs. (11) and (13).

5. Results

In order to illustrate the performance of the proposed modeling approach, two case studies are analyzed. The base case is the heuristic schedule of a given evaporation system of 14 units (Table 4). As a second case, the proposed re-design problem was solved for the same 14 units of the base case in order to generate an alternative evaporation structure to achieve an optimized performance. In other words, the same units of the base case were allowed to "reallocate" within the network to improve the evaporation work.

As performance criterion to compare both cases, the sum of the sugar concentrations in each unit of the evaporation system along the whole planning horizon is considered:

$$FO = \sum_{i=1}^{M}\sum_{j=1}^{NE_i}\sum_{t=1}^{T} x_{i,j,t} \tag{79}$$

As previously established, such performance index is appropriate for the sugarcane industry since it indirectly minimizes the overall steam consumption in the process. For comparison purposes, the distribution of steam between the evaporation and the crystallization sections will be also reported. For both cases, the steam required in the crystallization stage will be calculated from Eq. (74) with a product concentration (x_P) of 90%.

Since the cleaning tasks of each evaporation train require about 12 h, 28 periods of half a day were adopted in order to represent a two weeks planning horizon. Two cleaning stops are forced during that period in order to resemble the industrial practice of one cleaning shutdown per train per week.

A processing capacity of 700 t/h of a 16% sugar concentration juice was considered. The limit on the outlet concentration is the approach to saturation at which the crystallization process starts. In practice a concentration bound of 70% is recommended. Due to equipment limitations, the upper mass flow rate (F_i^{up}) fed to the each evaporation line is set in 400 t/h.

Each unit of a line has a different global heat transfer resistance and, hence, a particular linear equation is needed to represent its behavior. Slopes and y-intercepts for the units were calculated from plant data [17]. Global heat transfer resistance linear coefficients for an evaporation line of up to five units are shown in Table 5, where the first column corresponds to the y-intercept values for just cleaned units and the second one presents the slopes. Each line is considered to be at a different stage of its cycle at the beginning of the time horizon. The y-intercepts at the beginning of the time horizon are shown in Table 6.

5.1. Base case

Table 4 shows the configuration of the network corresponding to the base case, which constitutes an arbitrary arrangement of the available evaporation units. The adopted heuristic 14-day (28 periods) shutdown schedule implies the flow rate profile shown in Fig. 6. Such schedule comprises two identical 7-day cycles with an arbitrary cleaning scheme. It can be observed that the lines are shut down for maintenance in the following sequence: line 1 in periods 1 and 15, line 2 in periods 2 and 16, and line 3 in periods 3 and 17. One third of the total flow rate is assigned to each line when all three lines are operating. When one of the lines is shut down for cleaning, the corresponding flow rate is equally distributed among the remaining operating trains.

The corresponding objective function (Eq. (79)) was calculated for this heuristic system rendering 8339. The amount of steam required in the whole time horizon is 11,549 tons of which, 3243 correspond to the evaporation section and 8306 to the crystallization stage. The profiles for the different variables were also obtained. Since such profiles are similar to those for the optimized case (Figs. 7–15) they are not reproduced here. A detailed discussion of the behavior of the main variables is, however, presented in the following section based on the profiles corresponding to the optimized case.

5.2. Optimized case

The mathematical model was implemented in the GAMS language [18] and solved with the MINLP solver DICOPT++ [19]. CONOPT3 [19] and CPLEX [19] were adopted for the NLP and MIP sub-problems, respectively. The resulting MINLP model has 10,627 constraints, 3621 continuous variables, and 1182 binary variables. The solution was obtained in 469.5 CPU seconds on a Pentium IV personal computer with 448 MB of RAM.

Table 4
Network structure for base case.

		Evaporation units $A_{i,j}$ (m^2)				
		1	**2**	**3**	**4**	**5**
Lines	**1**	1500	800	800	800	700
	2	1500	700	700	700	650
	3	1500	1000	900	800	–

Table 5
Parameters of the global heat transfer resistances.

Unit	$R^0_{i,j}$ (hm^{2}C/kcal)	$C2_{i,j}$ (m^{2}C/kcal)
1	0.3487	0.0011
2	0.4163	0.0025
3	1.0866	0.0054
4	1.5377	0.0078
5	2.0435	0.0105

Table 6
y-intercepts for $R_{i,j}$ at the beginning of the time horizon.

		Evaporation unit $C1_{i,j}$ (hm^{2}C/kcal)				
		1	**2**	**3**	**4**	**5**
Lines	**1**	0.3619	0.4463	1.0618	1.445	2.1695
	2	0.3751	0.4763	1.1266	1.5386	2.2955
	3	0.3883	0.5063	1.1914	1.6322	2.4215
	4	0.4015	0.5363	1.2562	1.7258	2.5475

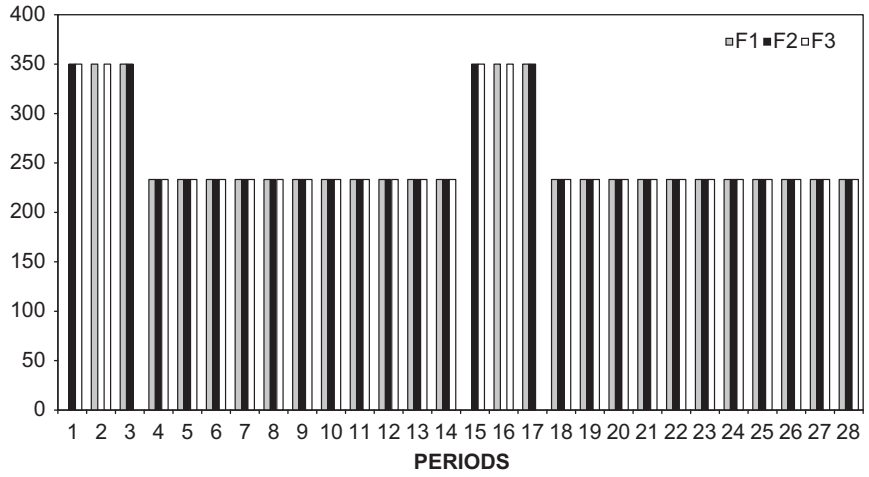

Fig. 6. Flow rates fed to the evaporation lines for the base case.

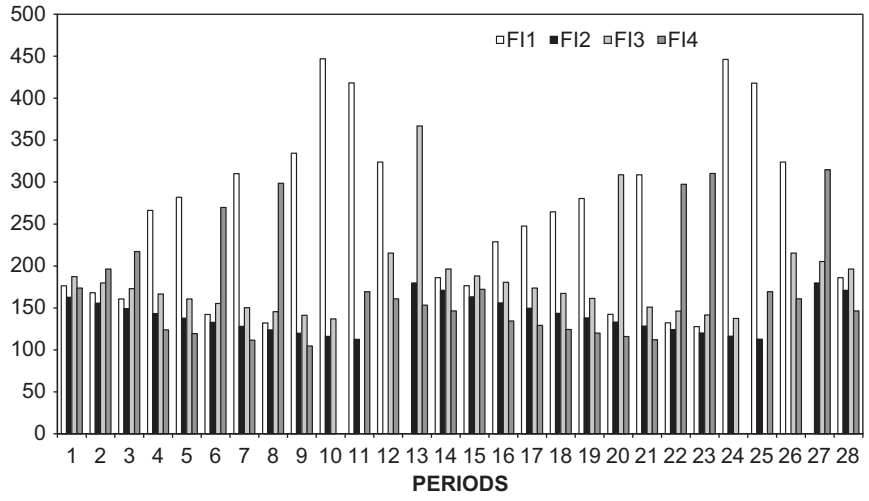

Fig. 7. Flow rates fed to the evaporation lines for optimized case.

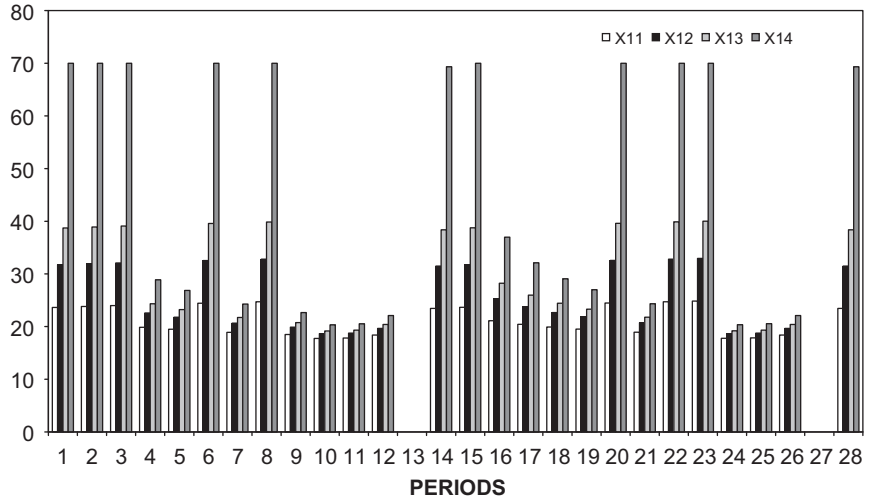

Fig. 8. Concentration profile for evaporation line 1.

The optimal structure shown in Table 7 has an objective function value (Eq. (79)) of 13,211. Note that the 14 available units were allocated in four lines. As expected, the objective function is better than that corresponding to the heuristic system (37% increase). For the whole time horizon, the steam amounts used in the evaporation and crystallization sections

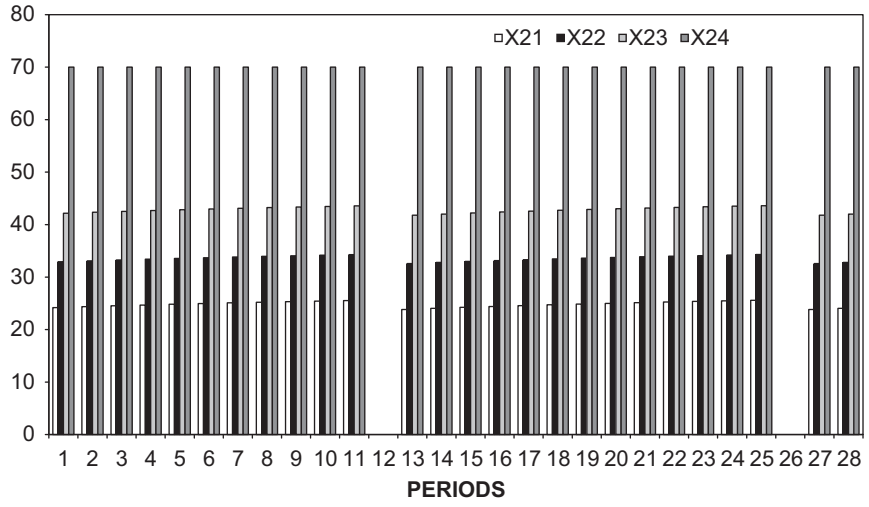

Fig. 9. Concentration profile for evaporation line 2.

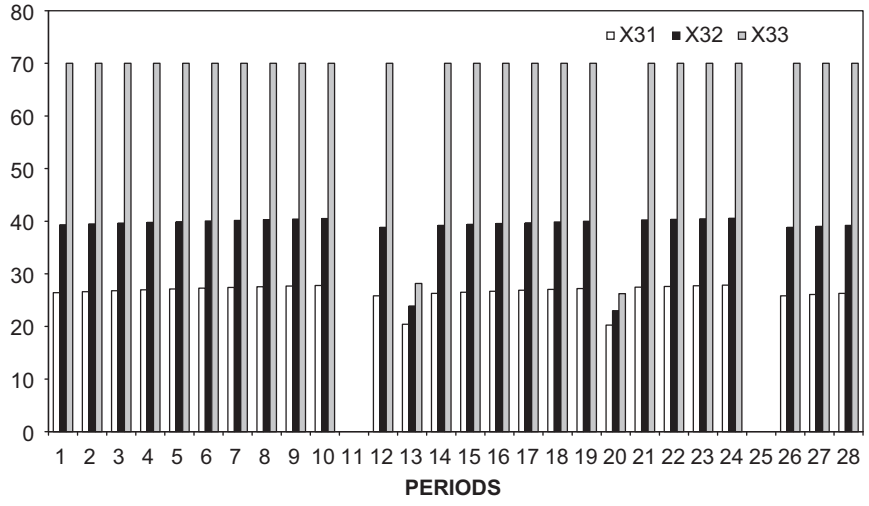

Fig. 10. Concentration profile for evaporation line 3.

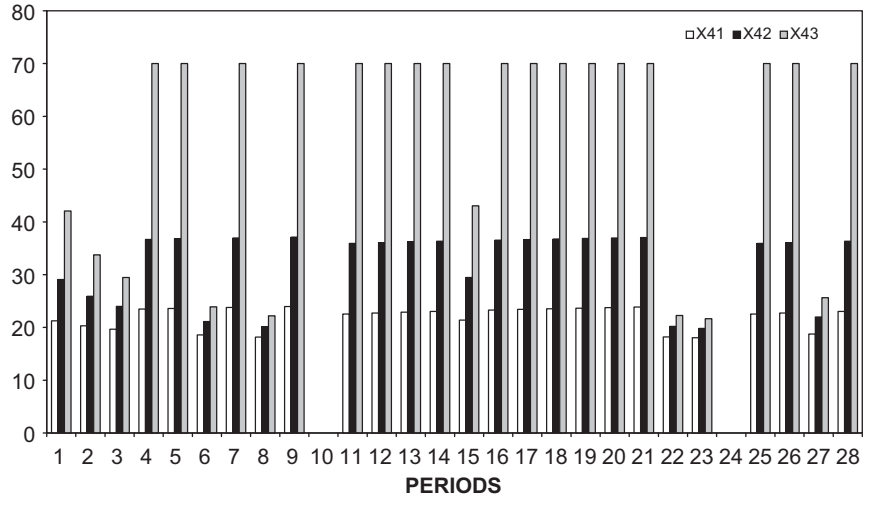

Fig. 11. Concentration profile for evaporation line 4.

were 5448 and 4296 tons, respectively. As expected, the steam needed to achieve a larger concentration at the evaporation section is larger than the corresponding to the base case (5448 tons vs. 3243 tons), but considering both operations together, the global amount of steam is lower in the optimized case (9744 tons vs. 11,549 tons).

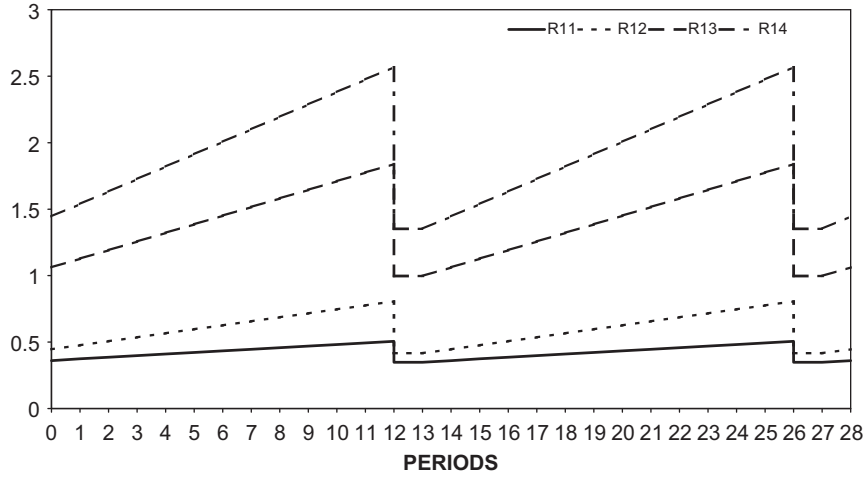

Fig. 12. Global heat transfer resistance for evaporation line 1.

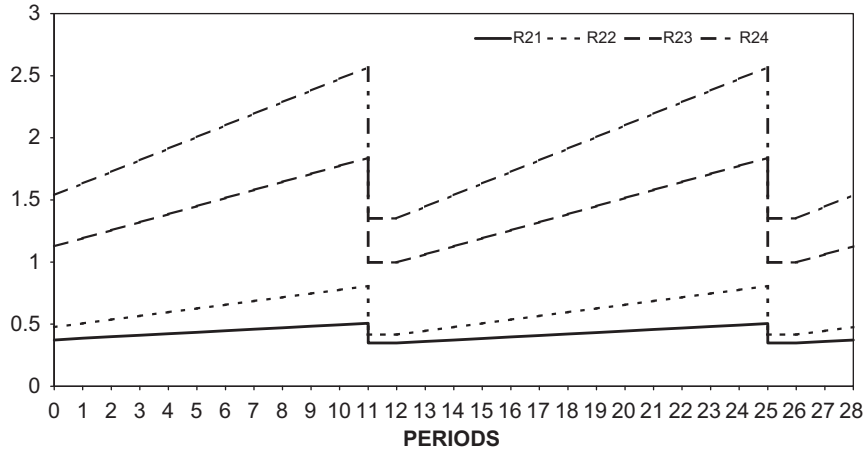

Fig. 13. Global heat transfer resistance for evaporation line 2.

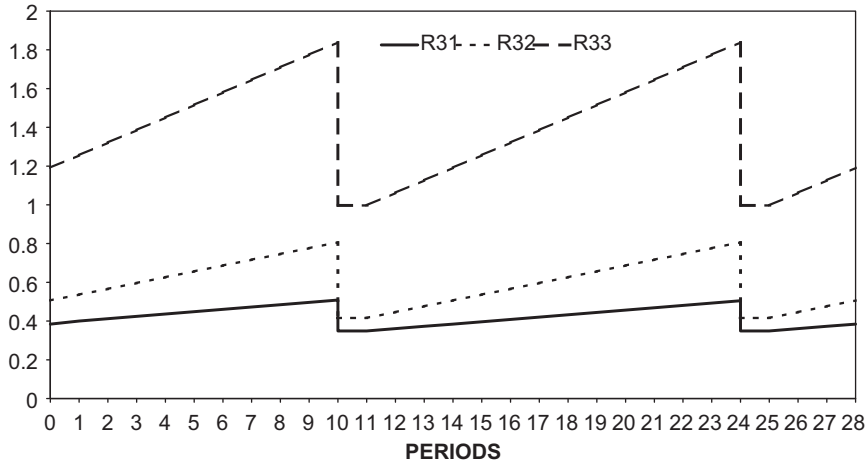

Fig. 14. Global heat transfer resistance for evaporation line 3.

While a significant improvement was obtained regarding the base case, the optimal solution is not necessarily the best possible, since the MINLP model is non-convex and local convergence solvers were used in the optimization.

Optimal values for the shutdown periods are shown in Table 8. Note that the model determines a cycle length for each evaporation line. This cycle length starts for line i at $TC_{1,i}+1$ and ends at $TC_{2,i}+1$, including operation and cleaning. All evaporation lines complete 2 cycles, hence, 2 shutdowns are performed as imposed by the model. As expected, no simultaneous shutdowns are performed for different evaporation lines.

The flow rates fed to the evaporation lines each time period are shown in Fig. 7. Note that the fed flow rates change from period to period in a rather erratic way. The reason of this

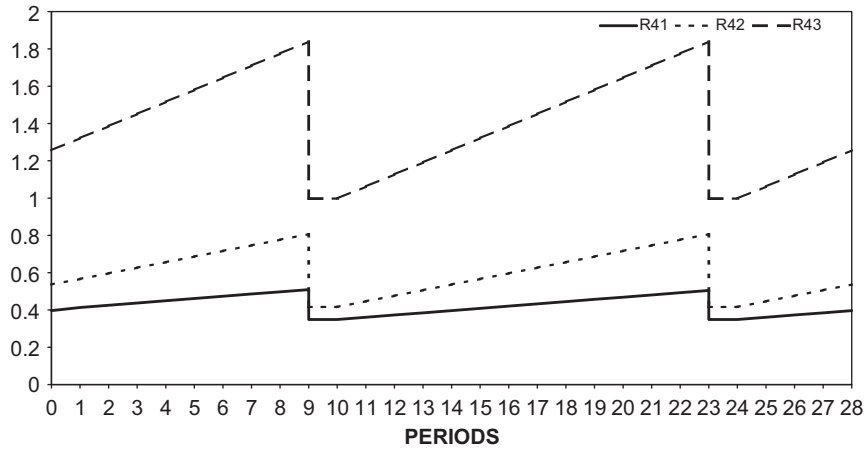

Fig. 15. Global heat transfer resistance for evaporation line 4.

Table 7
Optimal structure for the evaporation network.

		Evaporation units $A_{i,j}$ (m^2)			
		1	**2**	**3**	**4**
Lines	**1**	1500	800	700	1000
	2	1500	800	800	800
	3	1500	700	700	–
	4	900	700	650	–

Table 8
Optimal shutdown periods for the case study.

Line	$TC_{1,i}$	$TC_{2,i}$
1	12	26
2	11	25
3	10	24
4	9	23

behavior is that such flow rates are conveniently modified each time period to account for the heat resistance increase in the lines in order to optimize the adopted objective. In particular, when a certain line is shut down, the corresponding flow is best distributed within the remaining operating lines.

The effect of the varying flow rates can be appreciated in the concentration profiles (Figs. 8–11) where the outlet sugar concentrations of each unit of the series are reported. Note that the upper concentration bound (70%) is reached in many periods in the last units of the lines. However, in some lines in certain time periods, low final concentrations can be observed. See for example line 1 in periods 10, 11, and 12 (Fig. 8). In those periods, lines 4, 3, and 2 are shut down for cleaning, respectively, and most of the corresponding flow rate is diverted to line 1, which has the largest heat transfer surface. Therefore, low outlet concentrations are obtained in line 1 in those periods. Also note that for line 1, cleaning tasks are performed in period 13 (Fig. 8) and most of the corresponding flow rate is diverted to line 3.

The profiles of the global heat transfer resistances for the different evaporation lines along the time horizon are shown in Figs. 12–15. A dramatic reduction in the resistance is observed at periods when lines are shut down for maintenance. Maximum global heat transfer resistance obtained values were 0.5095, 0.8063, 1.8394, and 2.5682 ($h\,m^2\,^\circ C/kcal$), for units 1, 2, 3, and 4, respectively. The global heat transfer resistance value reached at the last period is identical to that at the beginning of the time horizon, thus, the cycle could be repeated over and over until the desired production is completed.

The amount of steam consumed at the different periods for both, the heuristic and the optimized cases, are shown in Fig. 16. The dashed bars correspond to the base case while the plain color bars to the optimized case. The bottom part of each bar represents the steam required by the evaporation section while the upper part corresponds to the crystallization stage. In many periods, the optimized network uses more steam for evaporation than the heuristic one (black vs. tight dashed). However, the integrated steam consumption is always lower for the optimized process.

6. Conclusions and future work

The integrated re-design and scheduling problem of systems of parallel multiple effect evaporation lines was addressed by means of a multi-period mixed integer nonlinear programming model. The formulation considers the decay in equipment performance with operating time due to fouling, which is a relevant feature in the operation of almost every heat transfer system where liquids are involved. To predict the global heat transfer resistance values, a linear model was adopted. In order to take into account the fouling severity due to increased concentration, the parameters of the linear model are considered to vary with the position of the heat exchanger in the network.

Steady state operation and no mass losses are reasonable model hypotheses since plants tend to operate in steady state condition and product loss avoidance is a permanent operational target in any industry. Also, the energy involved in the sensitive heat contribution is negligible compared to the latent heat component and, therefore, the increase of the boiling point is considered to have little incidence in the energy balances. The linear pressure drop among all evaporation units is justified by practical issues, for example in order to avoid withdrawals of juice. Maybe the strongest adopted assumption is that in the optimized case, the control system of the plant is considered to be able to tightly distribute the feed flow rate to each evaporation train according to the established schedule. Such level of automation might be rare in current evaporation plants and therefore the obtained solution could not be easily implemented in practice. However, our intent is to highlight the potential benefits of

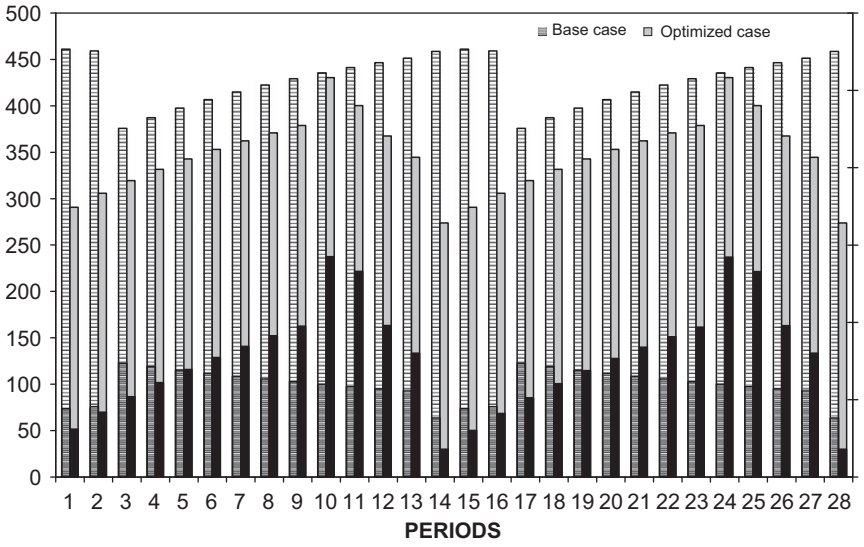

Fig. 16. Steam consumed for evaporation and crystallization operations.

working with an improved network arrangement and more sophisticated control systems.

The model determines the optimal structure of the evaporation system from a given number of evaporation units, together with the lines shutdown schedule to perform cleaning tasks in order to restore heat transfer efficiency. For every period of the time horizon, the model provides the flow rates fed to each line and the corresponding outlet flow rates, concentrations, steam consumption and vapor generation profiles.

In order to illustrate the performance of the model, a typical evaporation system of the sugarcane industry was considered. The results of a "base case" corresponding to a given network operated with a heuristic cleaning schedule and an "optimized case" were discussed in some detail. It was shown that by reallocating the available units within the evaporation matrix and wisely redistributing the flow rates fed to the lines, superior results can be obtained in terms of evaporation work, and therefore higher concentrations of product with the consequent energy savings.

A natural extension of the current contribution is the formulation of the "design and scheduling problem" of the evaporation network. Such a problem has to do with the configuration of the network from commercially available evaporators with the aim of optimizing an economic criterion involving capital and operative costs.

Additionally, a very challenging problem, of specific interest to the cane sugar industry, is the coordinated scheduling of the milling, the evaporation, and the crystallization stages. Since the milling and the crystallization operations are usually performed in parallel units, which have to be stopped for maintenance, there is a significant potential benefit resulting from the application of an integrated approach for the whole process.

Acknowledgment

This work was partially supported by the "Consejo de Investigaciones de la Universidad Nacional de Tucumán", "Consejo Nacional de Investigaciones Científicas y Técnicas de Argentina", and "Universidad Nacional del Sur".

References

[1] Epstein N. Optimum evaporator cycle with scale formation. Can J Chem Eng 1979;57:659–61.
[2] Casado E. Model optimizes exchanger cleaning. Hydrocarbon Process 1990;69(8):71–6.
[3] Sheikh AK, Zubari SM, Haq MU, Budair MO. Reliability-based maintenance strategies for heat exchangers subject to fouling. Trans ASME 1996;118:306–12.
[4] Georgiadis MC, Papageorgiou LG, Macchietto S. Optimal cyclic cleaning scheduling in heat exchanger networks under fouling. Comput Chem Eng 1990:S203–6.
[5] Georgiadis MC, Papageorgiou LG. Optimal energy and cleaning management in heat exchanger networks under fouling. Trans IChemE 2000;78(Part A):168–79.
[6] Heluane H, Sequeira S, Colombo MA, Hernandez MR, Graells M, Puigjaner L. Scheduling of continuous parallel lines in the evaporation section of sugar plants. Chem Eng Commun 2004;191:1121–46.
[7] Heluane H, Colombo M, Hernández MR, Graells M, Puigjaner L. Enhancing sugar cane process performance through optimal production scheduling. Chem Eng Proc 2007;46(3):198–209.
[8] Jain V, Grossmann IE. Cyclic scheduling of continuous parallel process units with decaying performance. AIChE J 2007;44:1623–36.
[9] Houze M, Juhasz N, Grossmann IE. Optimization model for production and scheduling of catalyst replacement in a process with decaying performance. In: Proceedings of the FOCAPO. 2003.
[10] Schulz EP, Bandoni JA, Diaz MS. Optimal shutdown policy for maintenance of cracking furnaces in ethylene plants. Ind Eng Chem Res 2006;45:2748.
[11] Hugot E. Manual para Ingenieros Azucareros. CIA Editorial Continental, México; 1982.
[12] Coulson JM, Richardson JF. Chemical Engineering. Pergamon Press; 1985.
[13] Georgiadis MC, Papageorgiou LG. Optimal scheduling of heat integrated multipurpose plants under fouling conditions. Appl Therm Eng 2001;21:1675–97.
[14] Ishiyama EM, Patterson WR, Wilson DI. Optimum cleaning cycles for heat transfer equipment undergoing fouling and aging. Chem Eng Sci 2011;66:604–12.
[15] Smaili F, Anfadi DK, Smaili F, Anfadi DK, Hatch CM, Herbert O, et al. Optimization of scheduling of cleaning in heat exchanger networks subject to fouling: sugar Industry case study. Trans IChemE 1999;77(Part C):159,164.
[16] Heluane H. Optimización de la operación de unidades continuas en paralelo en plantas agroindustriales. PhD thesis, FACET, Universidad Nacional de Tucumán, Argentina; 2010.
[17] Cárdenas G, Ruiz RM, Diez O, Aso G. Influencia del ensuciamiento en el coeficiente global de transferencia de calor en evaporadores. Int Sugar J 1995;97:1164S.
[18] GAMS: a users' guide. GAMS Development Corporation, 2008.
[19] GAMS: the solvers manual GAMS Development Corporation, 2008.